Disturbance Observer Based Model Prediction Control for a 2-DOF Nanopositioning Stage

Min Ming
School of Power and Mechanical Engineering
Wuhan University
Wuhan, China
mingmin_whu@whu.edu.cn

Zhao Feng
School of Power and Mechanical Engineering
Wuhan University
Wuhan, China
fengzhaozhao7@whu.edu.cn

Jie Ling
School of Power and Mechanical Engineering
Wuhan University
Wuhan, China
jamesling@whu.edu.cn

Xiaohui Xiao
School of Power and Mechanical Engineering
Wuhan University
Wuhan, China
xhxiao@whu.edu.cn

***Abstract*—To compensate the nonlinear effects of a nanopositioning stage and its model uncertainties, this paper presents a composite controller by integrating disturbance observer (DOB) and model prediction control (MPC). The nonlinearity and dynamic cross-coupling effects are treated as unknown disturbances to the system, and a DOB is used to partially estimate and compensate the disturbance to improved performance. A MPC is commonly used to track a reference signal, which minimizes the steady-state tracking error as well as increases the closed-loop bandwidth. Inspired by existing MPC schemes to improve the positioning performance of the piezo-actuated stage, a two-input two-output (TITO) form of the MPC controller is designed in this work with the estimated residual error being used to modify the reference in real time for better performance. The novelty of the proposed TITO MPC lies not only the compensation for nonlinear effects but also the rejection of cross-coupling dynamics effects in a 2-DOF nanopositioning system. The effectiveness of the proposed controller is validated through experimental investigations on a commercial nanopositioner platform. Experimental results show that the proposed method can improve the tracking performance of the piezo-actuated stage, compared to the traditional MPC.**

Keywords—Piezo-actuated stage, nonlinearity compensation, disturbance observer, model prediction control

I. INTRODUCTION

Nanotechnology is the study on the control or manipulation of matter on an atomic and molecular scale, and nanopositioning is one key branch of nanotechnology [1]. Nanopositioning stages have been widely applied in many precision instruments, such as nanomanipulators, scanning probe microscopes (SPMs), atomic force microscopes (AFMs), which are usually designed as flexure-hinge-guided mechanisms driven by piezoelectric actuators (PEAs) with the merits of small size, high positioning resolution and quick frequency response [2]. The use of flexure hinges makes it possible to eliminate the friction and clearance issues that exist in a traditional mechanism. However, the voltage actuation is dominantly used in practical applications, resulting in nonlinearity, particularly hysteresis effect. The hysteresis effect increasing with the amplitude and frequency of reference signal can greatly degrade the positioning accuracy [3]. The widely used proportional–integral–derivative (PID) controller in industry cannot provide satisfactory performance [4]. It is necessary to design more effective controllers to cope with the nonlinearity for precise positioning and tracking. There are various advanced control methods, such as robust resonant control (RRC) [5], iterative learning control (ILC) [6-8], adaptive control [9-10], repetitive control [11] and so on. The feedback-feedforward is integrated for control of a 2-DOF manipulation system in [12], while the data-based double-feedforward controller is designed to deal with a coupled parallel stage in [13].

In some larger stroke applications, hysteresis strongly compromises the accuracy of positioning [14], and it is necessary to take hysteresis into consideration. There are usually two methods: the first one is to build a hysteresis model and design a compensation controller based on the hysteresis model; the second one is to design the robust controller by treating hysteresis as interference. Typically, the hysteresis is modeled, and the feedforward control is completed based on the inverse hysteresis model [15-16] or the direct hysteresis model [17-18]. Although these controllers based on hysteresis models are direct and effective, the modeling and parameters identification are complex and computationally intensive. On the other hand, by treating the nonlinearity (including hysteresis, creep and model uncertainty) as interference, the design process of the robust controller is simple and practical. Slide mode control (SMC) [19] and model prediction control (MPC) [20] have recently attracted considerable attention as applied in the control of nanopositioning systems, both of which are simple to be implemented based on the identified nominal model.

As a variable structure control method, SMC is able to reject uncertainties and disturbances. However, chattering, caused by the discontinuous switching function in SMC, may excite the high-frequency resonant vibration, thereby degrading control performance and even damaging the actuators being controlled [21]. To solve this problem, in [22], a continuous integral

978-1-7281-4878-6/19/$31.00 ©2019 IEEE

terminal third-order SMC is designed to completely eliminate the chattering effect. And in [23], a PID regulator replaces the discontinuous switching function to eliminate chattering. Continuous SMC is usually used to deal with a second-order system and the digital slide mode control (DSMC) can only apply to a minimum phase system and is sensitive to the initial position error and noise. Among these algorithms, MPC algorithm is popular and widely adopted in the industrial process control [24]. It has been successfully applied to compensate for hysteresis nonlinearity of PEAs [20]. MPC can control the non-minimum system and deal with physical constraints in the generation of control actions. Compared to single-DOF nanopositioning systems, less research on the control of multi-DOF nanopositioning stages has been reported. In [25] and [26], a MPC is designed for a multi-axis piezo system with the system described by linear time-invariant (LTI) model. If the disturbance and uncertainties can be completely or partially estimated, such estimations should greatly facilitate their compensation by means of control. In literature, the active disturbance rejection approaches are developed for improving control performance. Reference [27] presents the development of a disturbance-observer-based (DOB) SMC for a 3-DOF nanopositioning stage. The MPC with disturbance observer (DOB) is proposed to control the current of raymond mill, which is a system with large time delays [24]. It is confirmed that DOB combined with feedback control can improve control performance for multi-axis system.

In reality, the challenge is that the identified nominal models of the commercially available multi-DOF nanopositioning stages are non-minimum phase. To raise to this challenge, this paper presents the development of a DOB-MPC for the 2-DOF piezo stage. Specifically, due to the imperfection of the DOB compensation, the tracking error including partial hysteresis and model uncertainties may exist. The residual error should be estimated and considered. This paper employs the difference value between the actual output and nominal model output to modify the reference in real time.

The rest of this paper is organized as follows: The design of the control is shown in Section II. Section III provides the experiment setup and identification of the system transfer function, and Section IV presents the experiment results. Finally, the paper is concluded in Section V.

II. DOB-MPC FOR THE 2-DOF NANOPOSITIONING STAGE

Fig. 1 shows the control scheme of the DOB-SMC for the 2-DOF nanopositioning stage. Specifically, the nonlinearity of the nanopositioning stage is estimated through the use of an observer and then compensated by means of the MPC with real-time modified reference.

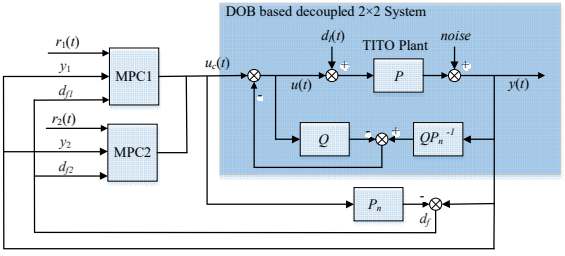

Fig. 1. Control scheme of the DOB-MPC for 2-DOF piezo system

A. Design of the Disturbance Observer

The block diagram of the standard DOB is shown in Fig. 2, where $P(z)$ is the real plant to be controlled and $P_n(z)$ is the nominal model, and $Q(z)$ is the low-pass filter. It can be seen that the procedure of the DOB closes a loop around the controlled plant to reject disturbances and force the input-output characteristics of this loop to approximate the nominal plant model. $P_n^{-1}(z)$ is the approximate inverse of the nominal model. The zero-phase-error tracking controller (ZPETC) technique is used to obtain the approximate inverse by converting NMP zeros of the model into stable zeros of the approximate inverse. $P(z)$ and $P_n(z)$ are chosen as diagonal transfer matrixes for the decoupling system.

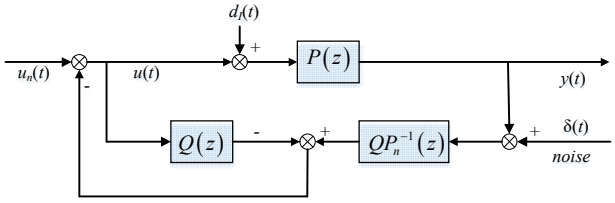

Fig. 2. The block diagram of the DOB

First, we write the dynamics of the system as in Eq. (1), partitioning $B(z)$ into the polynomial $B_s(z)$ containing the stable (invertible) zeros and the polynomial $B_u(z)$ containing the unstable (noninvertible) zeros:

$$P_n(z) = \frac{B(z)}{A(z)} = \frac{B_s(z)B_u(z)}{A(z)} \tag{1}$$

The polynomial $B_u(z)$ contains m unstable zeros. Then, the polynomial $B_f(z)$ contains m stable zeros is obtained by reflecting the roots z_i of $B_u(z)$ into the unit circle to $1/z_i$. According to the ZPETC, the inverse model is,

$$P_n^{-1}(z) = K\frac{A(z)B_f(z)}{B_s(z)} \tag{2}$$

$$K = 1\Big/\left(B_u(z)|_{z=1}\right)^2 \tag{3}$$

where, K is scalar that compensates for losses in the DC gain. For convenience, the variate z is omitted in the following.

It can be seen that P_n^{-1} is not causal. In this design, Q is specified as,

$$Q = Q_0 z^{-d} \tag{4}$$

In which, Q_0 is a low-pass filter with the unit gain at low frequencies and the delay d is the relative order between the numerator and the denominator of P_n^{-1}.

This ensures that $Q_0 P_n^{-1}$ is causal and the input signal and the estimated disturbance are coincident. The output of the plant can be expressed as follows,

$$y = P\left(u + d_I\right) = Pu + d \tag{5}$$

$$u = u_n - \left[QP_n^{-1}\left(y + \delta\right) - Qu\right] \tag{6}$$

B. MPC with Real-time Modified Reference

The MPC acts as a feedback controller and is used to generate the manipulated control increment sequence at each sample time by minimizing the difference between the desired output and the predictive output. Only the first move is applied to the plant and this step is repeated for the next sampling instance. The proposed composite control is shown in Fig. 1.

In this design, the nominal model of the plant is described by the state-space model as,

$$\begin{aligned} X\left(k+1\right) &= \mathbf{A}X\left(k\right) + \mathbf{B}U\left(k\right) \\ y\left(k\right) &= \mathbf{C}X\left(k\right) \end{aligned} \tag{7}$$

Making,

$$\begin{cases} \Delta X\left(k+1\right) = X\left(k+1\right) - X\left(k\right) \\ \Delta y\left(k+1\right) = y\left(k+1\right) - y\left(k\right) \\ \Delta U\left(k+1\right) = U\left(k+1\right) - U\left(k\right) \end{cases} \tag{8}$$

Eq. (7) can be rewritten as

$$\begin{cases} X_d\left(k+1\right) = \mathbf{A}_d X_d\left(k\right) + \mathbf{B}_d \Delta U\left(k\right) \\ y\left(k+1\right) = \mathbf{C}_d X_d\left(k\right) \end{cases} \tag{9}$$

where, $X_d(k+1) = [\Delta X(k+1)\ y(k)]$, $\boldsymbol{A}_d$, $\boldsymbol{B}_d$, $\boldsymbol{C}_\mathrm{d}$ are the augmented system matrices with $\mathbf{A}_d = \begin{bmatrix} \mathbf{A} & 0 \\ \mathbf{CA} & \mathbf{I} \end{bmatrix}$, $\mathbf{B}_d = \begin{bmatrix} \mathbf{B} \\ \mathbf{CB} \end{bmatrix}$, $\mathbf{C}_d = \begin{bmatrix} 0 & \mathbf{I} \end{bmatrix}$.

The predictive output sequence in the matrix form is then derived as,

$$Y = \mathbf{F}X_d\left(k\right) + \mathbf{\Phi}\Delta U \tag{10}$$

In which, $\mathbf{F} = \begin{bmatrix} \mathbf{C_d A_d} \\ \mathbf{C_d A_d}^2 \\ \vdots \\ \mathbf{C_d A_d}^{\mathbf{N_p}} \end{bmatrix}$,

$$Y = \begin{bmatrix} y\left(k+1\,|\,k\right) \\ y\left(k+2\,|\,k\right) \\ \vdots \\ y\left(k+N_p\,|\,k\right) \end{bmatrix},\ \Delta U = \begin{bmatrix} \Delta u\left(k\right) \\ \Delta u\left(k+1\right) \\ \vdots \\ \Delta u\left(k+N_c-1\right) \end{bmatrix}.$$

N_p, N_c are the prediction horizon and the control horizon respectively.

The DOB is designed based on the approximate inverse of the nominal model and the low-pass filter Q introduces the time delay d for the causality of the system. Partial disturbance still exists after the system with DOB. Considering the residual disturbance, the reference trajectory is modified in real time in the proposed method. The prediction model in MPC is the identified nominal model. The disturbance rejection performance is achieved without sacrificing the nominal tracking performance.

Considering the difference between the actual output with DOB compensation control and nominal model output, the residual error can be estimated and used to modify the reference in real time.

The residual disturbance,

$$d_f\left(k\right) = y\left(k\right) - P_n\left(k\right)u_c\left(k\right) \tag{11}$$

By assuming that the disturbance is slowly time-varying and bounded, then the future disturbance values sequence in prediction horizon is estimated by,

$$\zeta\left(k+1\right) = \begin{bmatrix} d_f\left(k\right) & \cdots & d_f\left(k\right) \end{bmatrix} \tag{12}$$

The modified reference is derived as,

$$R\left(k+1\right) = R_s\left(k+1\right) - \zeta\left(k+1\right) \tag{13}$$

where,

$$R_s = \begin{bmatrix} y_d\left(k+1\,|\,k\right) & y_d\left(k+2\,|\,k\right) & \cdots & y_d\left(k+N_p\,|\,k\right) \end{bmatrix}^T,$$

$$R = \begin{bmatrix} y_m\left(k+1\,|\,k\right) & y_m\left(k+2\,|\,k\right) & \cdots & y_m\left(k+N_p\,|\,k\right) \end{bmatrix}^T$$

Using the aforementioned notations, the cost function for minimization can be expressed by,

$$J = \left[Y - R\right]^T W_Y \left[Y - R\right] + \Delta U^T W_U \Delta U \tag{14}$$

In which, W_Y and W_U are the adjustable weight matrices.

III. System Description

When the modeling of nonlinearity is not required, the system can be represented by the equivalent system in Fig. 3 treating the hysteresis effect and model uncertainty as disturbance. The model of the piezo-actuated stage is shown in Fig. 3, where P represents the linear dynamics model. $u(t)$, $d(t)$,

$y(t)$ are the input voltage, unmeasurable disturbance, and displacement output respectively. The controller can be designed and completed for the linear dynamics model easily.

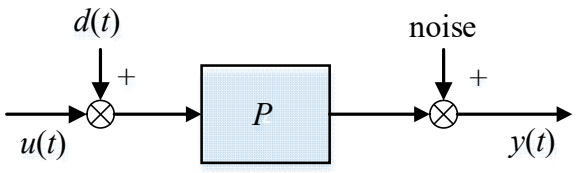

Fig. 3. The model of a piezo-actuated stage

A. Experimental Setup

The experimental setup is developed and shown in Fig. 4. According to Fig. 4(a), the setup is composed of a three-axis nanopositioner (P-561.3CD), a dSPACE MicrolabBox, a piezo amplifier module (E-503.00, Physik Instrumente) with a fixed gain of 10, a sensor monitor (E-509.C3A, Physik Instrumente) and the host PC. The control input voltage range is (0-10 V). And the output voltage range is (0-10 V), which is normalized with respect to 0-100μm. Details about the signal flow refer to Fig. 4(b). The control algorithm is designed in MATLAB/Simulink block diagram on the host PC, and then downloaded and executed on the target dSPACE MicroLabBox in the real-time software environment of dSPACE ControlDesk. When conducting experiments, the x-axis and y-axis are adopted to implement the proposed controller and the sample rate is set to 10 kHz.

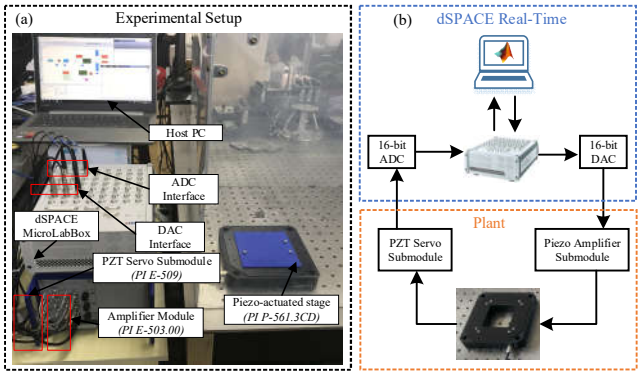

Fig. 4. The experimental setup of the piezo-actuated stage (a) Experimental platform (b) Block diagram of the signal flow

B. System Identification

Since only the nominal model is required in the proposed control design, the models are identified to describe the dynamics for x-axis and y-axis respectively. To obtain the model parameters, a sine-sweep input voltage with a constant amplitude of 200 mV between 0.1 Hz and 500 Hz is used as the input signal to both x-axis and y-axis. Notice that the low amplitude of the input voltage is used to excite the system for avoiding the effect of hysteresis nonlinearity. The input voltage and the output displacement data taken from the sensor are imported to MATLAB System Identification Toolbox to identify the models. The identified frequency response is shown in Fig. 5.

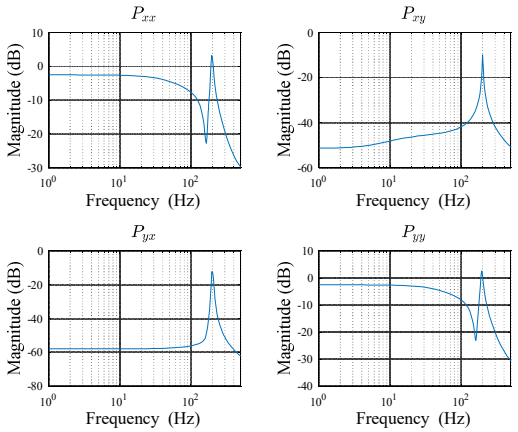

Fig. 5. Bode plot of the identified linear dynamics model

The positioning system can be described by the following equation:

$$P = \begin{bmatrix} P_{xx} & P_{xy} \\ P_{yx} & P_{yy} \end{bmatrix} \tag{15}$$

The discrete transfer functions of the x-axis and y-axis are,

$$P_{xx}(z) = \frac{0.0072654(z^2 - 1.982z + 0.9929)(z^2 - 2.256z + 1.316)}{(z - 0.9616)(z^2 - 1.91z + 0.9202)(z^2 - 1.977z + 0.9918)} \tag{16}$$

$$P_{yy}(z) = \frac{0.0064521(z^2 - 1.982z + 0.9926)(z^2 - 2.272z + 1.336)}{(z - 0.9627)(z^2 - 1.906z + 0.9164)(z^2 - 1.977z + 0.9917)} \tag{17}$$

IV. Experiments and Results

To illustrate the nanopositioning performance of the proposed TITO DOB-MPC controller compared with the TITO MPC controller in the time domain, circle signals of different frequencies are applied, which means that sinusoidal signal and cosine signal are used for x-axis and y-axis respectively. The motion tracking of circle signals with the frequency at 5 Hz, 10 Hz, and 20 Hz is tested respectively.

TABLE I. Tracking Error by RMS and MAX of the MPC and the Proposed DOB-MPC

Controller	*Frequency (Hz)*	*x axis (μm) RMS / MAX*	*y axis (μm) RMS / MAX*
MPC	5	0.1743 / 0.2781	0.1799 / 0.3266
	10	0.3538 / 0.5683	0.3651 / 0.6207
	20	0.8354 / 1.7030	0.8273 / 2.7747
DOB-MPC	5	0.0686 / 0.1351	0.0661 / 0.1118
	10	0.1513 / 0.3199	0.1408 / 0.2669
	20	0.4921 / 1.0227	0.4324 / 1.1485

For a clear presentation, Table 1 lists the value of RMS and MAX tracking errors with the MPC and the proposed DOB-MPC controllers. Compare with the traditional MPC, it can be

observed that the proposed DOB-MPC controller achieves satisfactory performance when tracking signals at different frequencies.

Fig. 6 shows the tracking performance with the amplitude at 30 μm and the frequency at 5 Hz, and the performance of tracking circle contour is presented in Fig.7. The root mean square (RMS) value of the tracking error of *x*-axis with traditional MPC is 0.1743 μm, whereas the RMS error with the proposed DOB-MPC is 0.0686 μm, which is a 60.6% improvement over MPC. Due to the DOB, the two axis are decoupled. The similar improvement of tracking performance can be seen for *y*-axis.

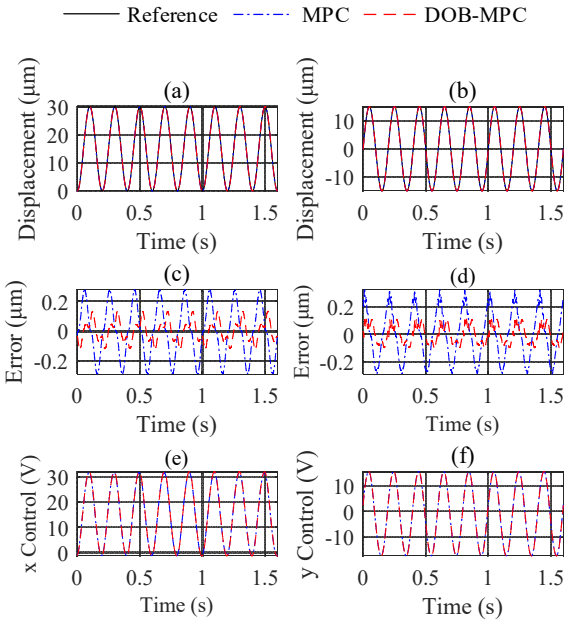

Fig. 6. Comparison of tracking performance of circle signal with the frequency at 5 Hz: (a) *x*-axis displacement, (b) *y*-axis displacement, (c) *x*-axis error, (d) *y*-axis error, (e)(f) control input for x and *y* axis

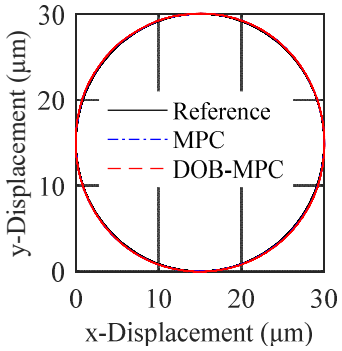

Fig. 7. Tracking performance of circle contour with the frequency at 5 Hz

Fig. 8 and Fig. 9 show the tracking performance with the amplitude at 30 μm and the frequency at 10 Hz.

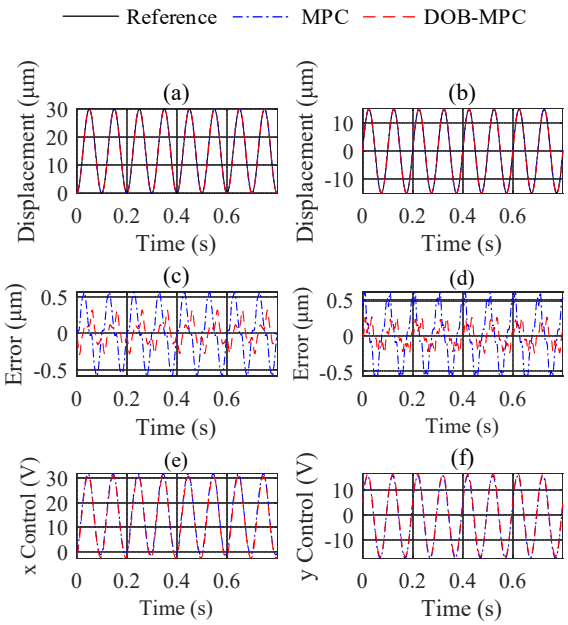

Fig. 8. Comparison of tracking performance of circle signal with the frequency at 10 Hz: (a) *x*-axis displacement, (b) *y*-axis displacement, (c) *x*-axis error, (d) *y*-axis error, (e)(f) control input for x and *y* axis

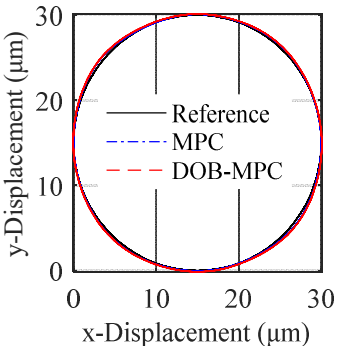

Fig. 9. Tracking performance of circle contour with the frequency at 10 Hz

It is also worthy of noting that the proposed DOB-MPC scheme can provide better performance of tracking at different frequencies than traditional MPC, but the improvement effect at high frequency is not as good as that at low frequency. As the amplitude and frequency of the tracking signal increase, the disturbance can't be assumed slowly time varying. According to the perturbation estimation technique, the disturbance is estimated by its one-step delayed value and is treated as a constant in prediction horizon, which is not enough accurate in applications for tracking signals of high frequency. And the performance is limited by the bandwidth of DOB.

V. Conclusion

This paper presents the development of a composite control for two input and two output piezo-actuated system. It enhances the performance of the MPC by adding a DOB and modifying the reference based on the residual disturbance. The DOB can observe and compensate the hysteresis nonlinearity and linear dynamic coupling at the same time. Due to the imperfection of

the DOB compensation, the residual error is used to modify the reference for better tracking performance. By using the proposed control frame, the nonlinearity and coupling between axes to be rejected by the feedback control is reduced and the control performance of the 2-DOF nanopositioning stage is greatly improved.

ACKNOWLEDGMENT

This work was supported by *Shenzhen Science and Technology Program* (grant JCYJ20170306171514468) and *China Postdoctoral Science Foundation* (grant 2018M642905).

REFERENCES

[1] P. R. Ouyang, R. C. Tjiptoprodjo, W. J. Zhang, and G. S. Yang, "Micromotion devices technology: The state of arts review," *The International Journal of Advanced Manufacturing Technology*, vol. 38, pp. 463–478, 2008

[2] G. Y. Gu, L. M. Zhu, C. Y. Su, H. Ding, and S. Fatikow, "Modeling and control of piezo-actuated nanopositioning stages: A survey," *IEEE Transactions on Automation Science and Engineering*, vol. 13, no. 1, pp. 313-332, 2016.

[3] Y. Cao, X. B. Chen, "A novel discrete ARMA-based model for piezoelectric actuator hysteresis," *IEEE/ASME Transactions on Mechatronics*, vol. 17, no. 4, pp. 737-744, 2012.

[4] H. Tang, and Y. Li, "Feedforward nonlinear PID control of a novel micromanipulator using Preisach hysteresis compensator," *Robotics and Computer-Integrated Manufacturing*, vol. 34, pp. 124-132, 2015.

[5] J. Ling, M. Rakotondrabe, Z. Feng, M. Ming, and X. Xiao, "A robust resonant controller for high-speed scanning of nanopositioners: design and implementation," *IEEE Transactions on Control Systems Technology*, 2019, unpublished.

[6] J. Ling, Z. Feng, D. Yao, and X. Xiao, "Non-linear contour tracking using feedback PID and feedforward position domain cross-coupled iterative learning control," *Transactions of the Institute of Measurement and Control*, vol. 40, no. 6, pp. 1970-1982, 2018.

[7] Z. Feng, J. Ling, M. Ming, and X. Xiao, "A model-data integrated iterative learning controller for flexible tracking with application to a piezo nanopositioner," *Transactions of the Institute of Measurement and Control*, vol. 40, no. 10, pp. 3201-3210, 2018.

[8] Z. Feng, J. Ling, M. Ming, and X. H. Xiao, "High-bandwidth and flexible tracking control for precision motion with application to a piezo nanopositioner," *Review of Scientific Instruments*, vol. 88, no. 8, 085107, 2017.

[9] S. Xiao, Y. Li, and J. Liu, "A model reference adaptive PID control for electromagnetic actuated micro-positioning stage," *in Automation Science and Engineering (CASE), 2012 IEEE International Conference on*, Aug. 2012, pp. 97-102.

[10] J. Ling, Z. Feng, M. Ming, and X. Xiao, "Model reference adaptive damping control for a nanopositioning stage with load uncertainties," *Review of Scientific Instruments*, vol. 90, no. 4, 045101, 2019.

[11] Z. Feng, J. Ling, M. Ming, and X. Xiao, "Integrated modified repetitive control with disturbance observer of piezoelectric nanopositioning stages for high-speed and precision motion," *Journal of Dynamic Systems, Measurement, and Control*, 2019.

[12] J. Ling, Z. Feng, M. Ming, and X. Xiao, "Precision contour tracking using feedback-feedforward integrated control for a 2-DOF manipulation system," *International Journal of Robotics & Automation*, vol. 33, no. 3, pp. 276-283, 2018.

[13] Z. Feng, J. Ling, M. Ming, and X. Xiao, "Data-based double-feedforward controller design for a coupled parallel nanopositioning stage," *Proceedings of the Institution of Mechanical Engineers, Part I: Journal of Systems and Control Engineering*, vol. 231, no. 10, pp. 881-892, 2017.

[14] W. Zhu, and D. H. Wang, "Non-symmetrical Bouc–Wen model for piezoelectric ceramic actuators," *Sensors and Actuators A: Physical*, vol. 181, pp. 51-60, 2012.

[15] G. Song, J. Zhao, X. Zhou, and J. A. De Abreu-García, "Tracking control of a piezoceramic actuator with hysteresis compensation using inverse Preisach model," *IEEE/ASME transactions on mechatronics*, vol. 10, no. 2, pp. 198-209, 2005.

[16] S. Rosenbaum, M. Ruderman, T. Strohla, and T. Bertram, "Use of Jiles–Atherton and Preisach hysteresis models for inverse feed-forward control," *IEEE Transactions on Magnetics*, vol. 46, (12), 3984-3989, 2010.

[17] M. Rakotondrabe, "Bouc–Wen modeling and inverse multiplicative structure to compensate hysteresis nonlinearity in piezoelectric actuators," *IEEE Transactions on Automation Science and Engineering*, vol. 8, no. 2, pp. 428-431, 2011.

[18] Q. Xu, "Identification and compensation of piezoelectric hysteresis without modeling hysteresis inverse," *IEEE Transactions on Industrial Electronics*, vol. 60, no. 9, pp. 3927-3937, 2013.

[19] J. P. Mishra, Q. Xu, X. Yu, and M. Jalili, "Precision position tracking for piezoelectric-driven motion system using continuous third-order sliding mode control," *IEEE/ASME Transactions on Mechatronics*, vol. 23, no. 4, pp. 1521-1531, 2018.

[20] M. S. Rana, H. R. Pota, and I. R. Petersen, "Performance of sinusoidal scanning with MPC in AFM imaging," *IEEE/ASME Transactions on Mechatronics*, vol. 20, no. 1, pp. 73-83, 2015.

[21] S. Mobayen, and D. Baleanu, "Stability analysis and controller design for the performance improvement of disturbed nonlinear systems using adaptive global sliding mode control approach," *Nonlinear Dynamics*, vol. 83, no. 3, pp. 1557-1565, 2016.

[22] Q. Xu, "Continuous integral terminal third-order sliding mode motion control for piezoelectric nanopositioning system," *IEEE/ASME Transactions on Mechatronics*, vol. 22, no. 4, pp. 1828-1838, 2017.

[23] J. Y. Peng, and X. B. Chen, "Integrated PID-based sliding mode state estimation and control for piezoelectric actuators," *IEEE/ASME Transactions on Mechatronics*, vol. 19, no. 1, pp. 88-99, 2014.

[24] D. Niu, X. Chen, J. Yang, X. Wang and X. Zhou, "Composite control for raymond mill based on model predictive control and disturbance observer.," *Advances in Mechanical Engineering*, vol. 8, no. 3, 1687814016639825, 2016.

[25] L. Cavanini, M. L. Corradini, G. Ippoliti, and G. Orlando, "A model predictive control for a multi-axis piezo system: development and experimental validation," *in Decision and Information Technologies (CoDIT), 2017 4th International Conference on Control*, Apr. 2017, pp. 0067-0072.

[26] M. S. Rana, H. R. Pota, and I. R. Petersen, "Nanopositioning performance of MIMO MPC," *in 2015 10th Asian Control Conference (ASCC)*, May 2015, pp. 1-6.

[27] Y. Cao, and X. B. Chen, "Disturbance-observer-based sliding-mode control for a 3-DOF nanopositioning stage," *IEEE/ASME Transactions on mechatronics*, vol. 19, no. 3, pp. 924-931, 2014.